Case Studies in Thermal Engineering 8 (2016) 164–175

Contents lists available at ScienceDirect

Case Studies in Thermal Engineering

journal homepage: www.elsevier.com/locate/csite

Thermal performance of two heat exchangers for thermoelectric generators

W. Li [a,*], M.C. Paul [a], J. Siviter [a], A Montecucco [a], A.R. Knox [a], T. Sweet [b], G. Min [b], H. Baig [c], T.K. Mallick [c], G. Han [d], D.H. Gregory [d], F. Azough [e], R. Freer [e]

[a] School of Engineering, University of Glasgow, Glasgow G12 8QQ, UK
[b] School of Engineering, Cardiff University, Cardiff CF24 3AA, UK
[c] The Environment and Sustainability Institute, University of Exeter, Penryn TR10 9FE, UK
[d] WestCHEM, School of Chemistry, University of Glasgow, Glasgow G12 8QQ, UK
[e] School of Materials, University of Manchester, Manchester M13 9PL, UK

ARTICLE INFO

Article history:
Received 21 April 2016
Received in revised form
8 June 2016
Accepted 21 June 2016
Available online 22 June 2016

Keywords:
Heat exchanger
CFD modelling
Thermoelectric generator
Heat transfer
Thermal and hydraulic performances

ABSTRACT

The thermal performance of a heat exchanger is important for the potential application in an integrated solar cell/module and thermoelectric generator (TEG) system. Usually, the thermal performance of a heat exchanger for TEGs is analysed by using 1D heat conduction theory which ignores the detailed phenomena associated with thermo-hydraulics. In this paper, thermal and momentum transports in two different heat exchangers are simulated by means of a steady-state, 3D turbulent flow k-ε model with a heat conduction module under various flow rates. In order to simulate the actual working conditions of the heat exchangers, a hot block with an electric heater is included in the model. The TEG module is simplified by using a 1D heat conduction theory, so its thermal performance is equivalent to a real TEG. Natural convection effects on the outside surfaces of the computational domains are considered. Computational models and methods used are validated under transient thermal and electrical experimental conditions of a TEG. The two heat exchangers designed in this paper have better thermal performance than an existing heat exchanger for TEGs. More importantly, the fin heat exchanger is more compact and efficient than the tube heat exchanger.

1. Introduction

The thermal performance of a heat exchanger, which is important for an integrated solar cell/module and thermoelectric generator (TEG) system, has been paid little attention to date. From a comprehensive literature review, it is found that the performance analysis of a heat exchanger for TEG application is usually done by using a simple 1D heat conduction theory. For example, free convection heat transfer and heat conduction in a flat-plate heat exchanger of TEG for an ocean thermal energy conversion (OTEC) system was analysed by Henderson [1] with a 1D heat transfer theory. Consequently, the heat exchanger-TEG system performance was investigated and a relationship between the TEG element area-to-length ratio and the temperature difference across the TEG and resulting electric power generation was obtained. Likewise, the thermal performance of a parallel-plate heat exchanger was calculated by Yu and Zhao [2]. As a result of this, the TEG performance

* Corresponding author.
E-mail addresses: Wenguang.Li@Glasgow.ac.uk (W. Li), Manosh.Paul@Glasgow.ac.uk (M.C. Paul).

http://dx.doi.org/10.1016/j.csite.2016.06.008
2214-157X/

associated with the exchanger was predicted analytically, and the heat exchanger-TEG system performance was explored further by means of a parametric study. Again by employing a basic 1D heat transfer model, three types of heat exchanger such as spiral, zig-zag and straight fin geometries for the TEG's cold and hot sides were investigated by Esarte et al. [3]. The overall heat transfer coefficient for the heat exchanger-TEG system was found to be 2.07 W/°C, 2.094 W/°C and 1.72 W/°C, respectively. Particularly, for the spiral heat exchanger, experiments were carried out to confirm the analytical temperature difference across the TEG module at varying water flow rate. As evidenced, this 1D simulation method may provide useful information but clearly ignores the effects associated with combined thermal and hydraulic occurrences within systems.

Recently, computational fluid dynamics (CFD) methodology has been applied to characterise the thermal performance of various heat exchangers such as plate, shell and tube, vertical mantle, compact and printed circuit board exchangers and also to optimize their design configurations (e.g. see Bhutta et al. [4]). It was pointed out that CFD has emerged as a cost effective tool to speed up the investigation of various heat exchanger designs as well as their hydraulic and thermal performances. It has also been noticed that the k-ε turbulence model has been extensively employed and an accuracy of 2–10% has generally been achieved against experimental data [4]. For example, a plate heat exchanger with undulated surfaces was optimized with a CFD package, ANSYS CFX 10.0, as well as with a response surface method conducted by Kanaris et al. [5]. Their chosen computational model was a 3D narrowed channel with inclined triangular undulations in herringbone pattern. The design variables included a blockage ratio, channel aspect ratio, corrugation aspect ratio, angle of attack and Reynolds number. The objective function was a linear combination function of heat transfer augmentation and pressure drop.

A method was also developed by Karmo et al. [6] to design an effective finned heat exchanger. The tube cross-sectional and longitudinal shapes were changed so that the angle between the fins and the tubes was on longer orthogonal. Various configurations were analysed using the CFD code, Fluent, to identify an optimal design. Recently, elliptical finned-tube heat exchanger thermal-hydraulic performance was optimized by using Fluent and response surface method based on seven design variables proposed by Sun and Zhang [7]. It was found out that a slightly increased axis ratio of elliptical tube section can improve the thermal-hydraulic performance at a higher air velocity outside the tubes or lower water flow rate in the tubes.

However, the literature also suggests that the CFD analysis leading to design and performance optimization of heat exchanger for TEGs is very limited. A hybrid TEG/thermal system with a radiation concentrator was proposed recently by Urbiola and Vorobiev [8]. An optimal configuration of the flat plate heat exchanger placed in the cold side of TEG was identified by using COMSOL Multiphysics software, and results showing the thermal energy stored in cooling water around 50 °C at midday. Most recently, TEGs and heat exchangers have been simulated by Sarhadi et al. [9] with the same software (COMSOL) and particularly the TEG arrangements layouts were investigated. The TEGs are considered to be a solid body, and the oil flows in the exchanges are considered to be laminar. Thermal contact resistance is also included in the interfaces between the TEGs and exchangers. However, the cooling oil flow rate is assumed to be distributed uniformly from one finned cannel to another.

In this contribution, the thermal performance of two heat exchangers on the cold side of a TEG is studied by means of ANSYS 15.0 CFX to identify their optimal configuration. The computational model includes a hot block-electrical heater, a TEG, a cold block-heat exchanger which maintains the TEG cold side to be in lower temperature. Since CFX is unable to deal with electrical modelling, the real TEG is represented by a thermal equivalent TEG with the same geometrical size. The heater is subject to the highest temperature, and cooling water at the exchanger inlet is kept at 19 °C. Natural convection effects on the outside surfaces of the computational domains due to environmental effects are considered. Water flow in the heat exchangers is turbulent, so turbulent eddy shear stresses are modelled by means of a k-ε turbulence model.

2. Computational models and methods

2.1. Computational models

Two heat exchangers are designed, one is a tube exchanger and the other is a fin exchanger, as shown in Fig. 1. Obviously, the fin heat exchanger is more compact than the tube exchanger. The heat exchanger is firmly attached to the top surface of a TEG by a pressure load. The water flow in the exchanger absorbs the heat discharged by the TEG when it generates electric power. The TEG is heated underneath through its substrate by an electrical heater inside the hot block. As a result, the interface between the exchanger and the TEG is kept at a lower temperature, but the interface between the hot block and the TEG is at a higher temperature. Eventually, a temperature difference is established between both sides of the TEG and electrical power is generated. To deal with an uneven distribution of temperature on the interfaces between the TEG and both the hot block and heat exchanger, three components must be considered simultaneously in a heat transfer simulation.

The TEG structure is simplified to a solid structure so as to make the heat transfer analysis easy, see Fig. 2. This simplified structure keeps its thermal behaviour being equivalent to the TEG based on a 1D heat conduction theory illustrated by Incropera et al. [10]. In the simplification, a few assumptions are made: (1) the materials of each component of the TEG are homogenous and their thermal resistance, heat specific capacity and density are constant and independent of temperature; (2) the thermal contact effect inside the TEG and on the interfaces between both the heater and heat exchanger and the TEG are negligible; (3) the effects of the air inside the TEG on the free heat convection and the equivalent density of the TEG are not taken into account. The heat conductivity of the copper straps is two-orders of magnitude larger than those of the legs and substrates, thus the heat resistance in the copper straps is also ignored. Additionally, the copper straps are as thin as 0.2 mm, so their contribution to the equivalent density of the TEG is excluded.

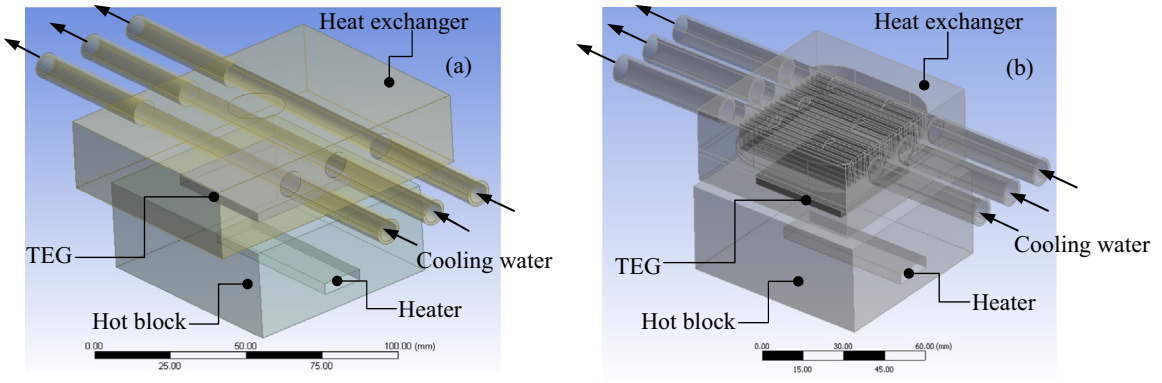

Fig. 1. Design of two heat exchangers for TEG, (a) tube exchanger (b) finned heat exchanger.

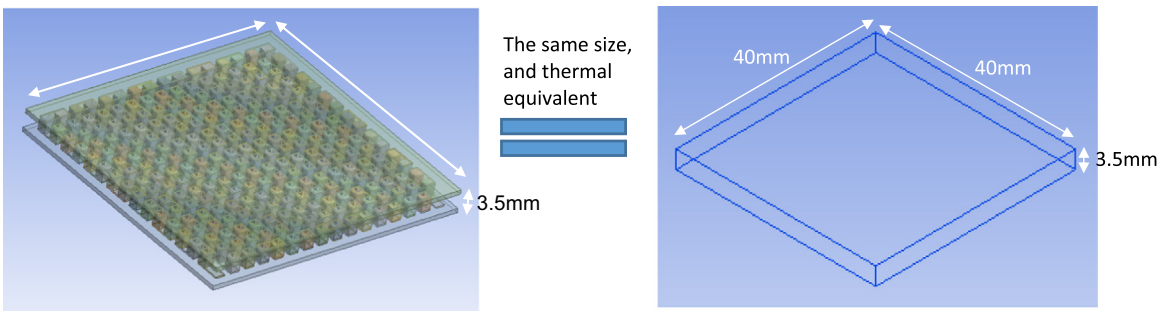

Fig. 2. TEG (left) and its thermal equivalent counterpart (right).

Bearing these assumptions in mind, the following thermal variables are obtained to describe the thermal equivalent counterpart of the TEG. The equivalent density of the TEG,

$$\rho_{eq} = \frac{2m_1 + nm_2}{A_1 h_1} \tag{1}$$

The equivalent conductivity of the TEG,

$$k_{eq} = \frac{1}{\frac{A_1}{nk_2A_2} + \frac{2}{k_1}} \tag{2}$$

The specific heat capacity of the TEG,

$$c_{p,eq} = \frac{1}{\frac{m}{nc_{p2}m_2} + \frac{2m}{c_{p1}m_1}} \tag{3}$$

where A_1 is the area of the ceramic substrates/plates, 40×40 mm^2; A_2 is the area of the legs, 1.4×1.4 mm^2; c_{p1} is the specific heat capacity of the substrates, 419 J/(kg K); c_{p2} is the specific heat capacity of the legs, 200 J/(kg K); $c_{p,eq}$ is the equivalent specific heat capacity of the TEG, 55.36 J/(kg K); h_1 is the total thickness of the TEG, 3.5 mm; h_2 is the length of the legs in the TEG, 1.8 mm; k_1 is the thermal conductivity of the substrates in the TEG, 31 W/(m K); k_2 is the thermal conductivity of the legs in the TEG, 1.6 W/(m K); k_{eq} is the equivalent thermal conductivity of the TEG, 0.4844 W/(m K); $m$is the total mass of the TEG without copper straps, $m = 2m_1 + nm$, kg; m_1 is the mass of one substrate, $m_1 = \rho_1 A_1 h_1$, kg; m_2 is the mass of total legs, $m_2 = n\rho_2 A_2 h_2$, kg; n is the number of legs in the TEG; ρ_1 is the density of substrate, 3220 kg/m^3; ρ_2 is the density of legs, 7440 kg/m^3; and ρ_{eq} is the equivalent density of the TEG, 2343.55 kg/m^3.

The thermal property constants of hot block, heat exchanger and cooling water that will be used in the heat transfer simulation have been listed in Table 1, including those of the equivalent TEG.

Since a steady-state thermal performance of heat transfer is investigated here, only the steady heat transfer and water flow, i.e. a conjugate heat transfer is simulated. The governing equations of the heat transfer simulation include the steady-state conservation equations of energy in the solid and fluid domains and the Navier-Stokes equations in the fluid domain. The cooling water flow is steady-state but 3D and turbulent. So, the standard k-ε turbulence model is chosen to handle turbulent shear stresses. A scalable wall function is adopted to treat the near wall boundary layer effect. The detailed information about these governing equations, flow model and wall function can be found in ANSYS [11].

Table 1
Thermal properties of components of heat exchangers used in heat transfer simulation.

Component	Material	Density (kg/m^3)	Specific heat capacity (J/(kg K))	Thermal conductivity k (W/(m K))
Hot block	Copper	8300	385	401
Heat exchanger				
Cooling water	25 °C water	997.05	4.18	0.58
Equivalent TEG	Combination of ceramic and Bi_2Te_3	2343.55	55.36	0.4844

2.2. Computational methods

The computational domains include the solid domains (hot block, heat exchanger case, fins, inlet and outlet pipes and TEG) and the fluid domain (cooling water). At first, the computational geometrical models are generated in SolidWorks® and then read by the ANSYS Design Modeler. Subsequently, the geometrical models are meshed using the ANSYS mesh generator. The number of mesh cells used in the tube exchanger and in the fin exchanger are 1.66 and 2.22 million, respectively, see Fig. 3(a) and (b). A tetrahedral mesh is generated in the solid domains of the heat exchanger and the hot block as well as in the fluid domains, however a hexahedral mesh is created in the solid domain of the TEG. Due to the difference

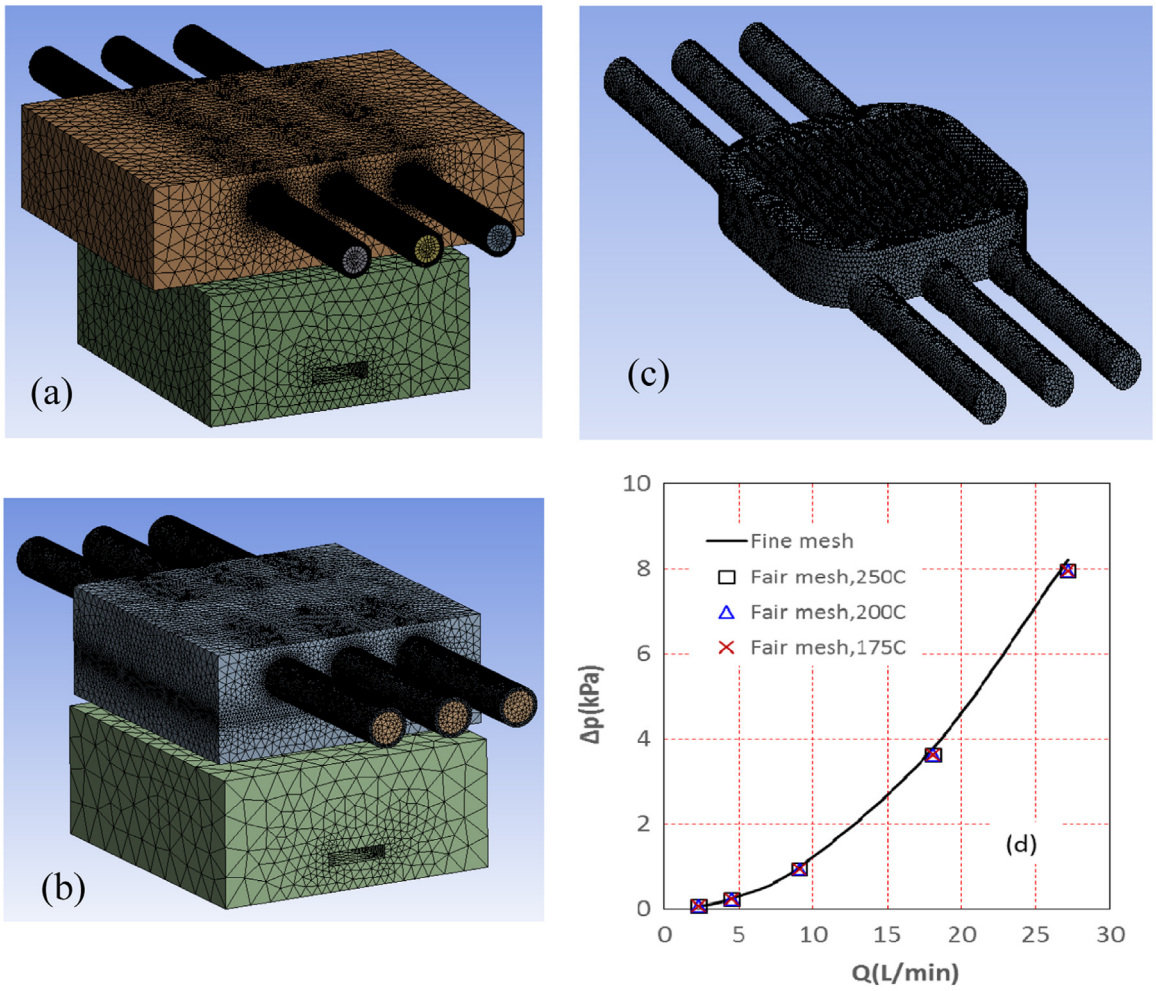

Fig. 3. Mesh patterns of two heat exchangers and isolated fluid domain, (a) tube exchanger, (b) fin exchanger, (c) fine mesh on isolated fluid domain, (d) pressure drops predicted by using mesh shown in (b) and (c).

in the linear dimensional scale, the mesh at the inlet and outlet tubes of heat exchanger is not fine enough, but is adequate for heat transfer analysis.

The minimum and maximum mesh sizes of the tetrahedral mesh in the complicated fluid domain of the fin exchanger are 0.05 mm and 3 mm respectively, and the growth rate from the minimum size increasing to the maximum is 1.2. The skewness of the mesh is in a range of 0–0.9 with a mean value of 0.26, while the orthogonal quality is in the range 0.13–0.99 with an average value of 0.84.

To identify the effects of mesh size on fluid flow, initially, the fluid domain is isolated and a fine mesh of 293 k cells is generated, as shown in Fig. 3(c). The fluid flow in that domain alone is simulated at three different heater temperatures (175 °C, 200 °C and 250 °C). The pressure drop across the domain is compared with those obtained with the mesh presented in Fig. 3(b). It is shown that if the water flow rate through a heat exchanger is less than 10 L/min, the pressure drop estimated with the two sets of mesh is nearly the same. The water flow rate for a TEG is usually considered to be within the range of 0.5–4.5 L/min, so the mesh size chosen for the fluid domain seems reasonable from an engineering perspective.

Secondly, a series of heat transfer and fluid flow boundary conditions are specified on the solid and fluid domains boundaries. At the entrance to the inlet tubes of the heat exchanger, an inlet velocity is applied, which has been calculated from the given water flow rate in a range of 0.5–4.5 L/min. In [12], the experimental flow rate was 1.02 L/min, but it has been extended here to cover a wide range of the flow rate e.g. 0.5–4.5 L/min. Note that there is an interface generated between the water and the solid domain in the heat exchanger, so the heat flux across the interface is conserved simultaneously. No slip velocity and hydraulic smooth boundary conditions are held on the wet walls. The temperature of water at the inlets of the heat exchangers is kept constant at 19 °C.

In addition, the end surfaces of the inlet and outlet tubes are adiabatic. All the other surfaces exposed to air are subject to free heat convection with a free heat transfer coefficient taken as 10 W/(m^2 K) [10]. The five surfaces of the cavity accommodating the electrical heater are assigned to be a constant temperature, namely 175 °C or 200 °C or 250 °C in the simulations. These temperatures can result in 100 °C, 150 °C and 200 °C temperature differences across the TEG, respectively, which are similar to those used in the experiments in [13] and [12]. The four side surfaces, bottom of the hot block are insulated and the ambient temperature is 19 °C [12]. Radiative transfer from the heat exchanger, TEG and hot block to the air is not taken into account as the effect is deemed to be negligible.

Finally, the heat transfer analyses in two heat exchangers are launched in ANSYS 15.0 CFX by means of a 3D, steady-state, turbulent flow model with heat conduction module under various flow rates. A high resolution advection scheme and a second-order diffusion scheme are adopted. The root mean squared tolerance residuals for convergence are specified to be 1×10^{-5}.

3. Results and discussion

3.1. Validation

At first, the physical model and numerical methods are validated using the experimental data in [12], in which a series of experimental data of the electric performance for a TEG were presented when the heater was subject to transient and steady temperatures, respectively. The experimental setup is illustrated in Fig. 4(a), and further, details are given in [13].

We have carried out a transient heat transfer simulation in CFX when the heater and water at the tube heat exchanger inlet are subject to the measured temperature profiles, as shown in Fig. 4(b), and the water is subject to 1.02 L/s flow rate. In the simulation, the material properties in Table 1, geometrical model, thermal and fluid flow models and the numerical methods in Section 2 are used, but the steady fluid flow models are switched to the transient ones. Two monitoring points are arranged each at the geometrical centre of the interface between the TEG cold side, and the centre of the interface between the TEG and the hot block to record the transient temperature profiles in the interfaces. Further, an additional three points are set at the outlet cross-section centre of the three tubes in the exchangers to show the temperature of water at the three outlet tube exits.

The temperature predicted on the cold side of the TEG is shown in Fig. 4(c). The predicted temperature follows the heater temperature history very closely. The difference between the prediction and measurement varies in the range of 0.5–2 °C, suggesting the computational models and methods used are feasible for simulating the thermal fluid dynamics in the heat exchanger. The maximum error occurs in 3000–3400 s time intervals where the electrical current applied is reduced and increased rapidly, see Fig. 5. This rapid change in the current can alter the Joule heat generated in the TEG legs significantly. The enlarged Joule heat at a higher current will raise the cooling water temperature.

The temperature of water at the three outlets of the heat exchanger is compared with those at the two outlets measured in Fig. 4(d). The temperatures at the three outlet tubes obtained by CFX are very close to each other and they are averaged and plotted for the two heat exchangers. The experimental temperature was slightly noisy after 1500 s because there was a rapid change in the TEG electric current applied. In general, the error in the water temperature between the prediction and the measurement is less 0.5 °C. The temperature of the TEG cold side is around 10 °C higher than the cooling water at the exchange inlet, indicting the performance of the tube heat exchanger is less efficient.

In addition, the same thermal transient analysis is conducted on the fin heat exchanger and the corresponding results are presented in Fig. 4(c) and (d). It is seen that the TEG cold side temperature is only 2 °C higher than that of the cooling water

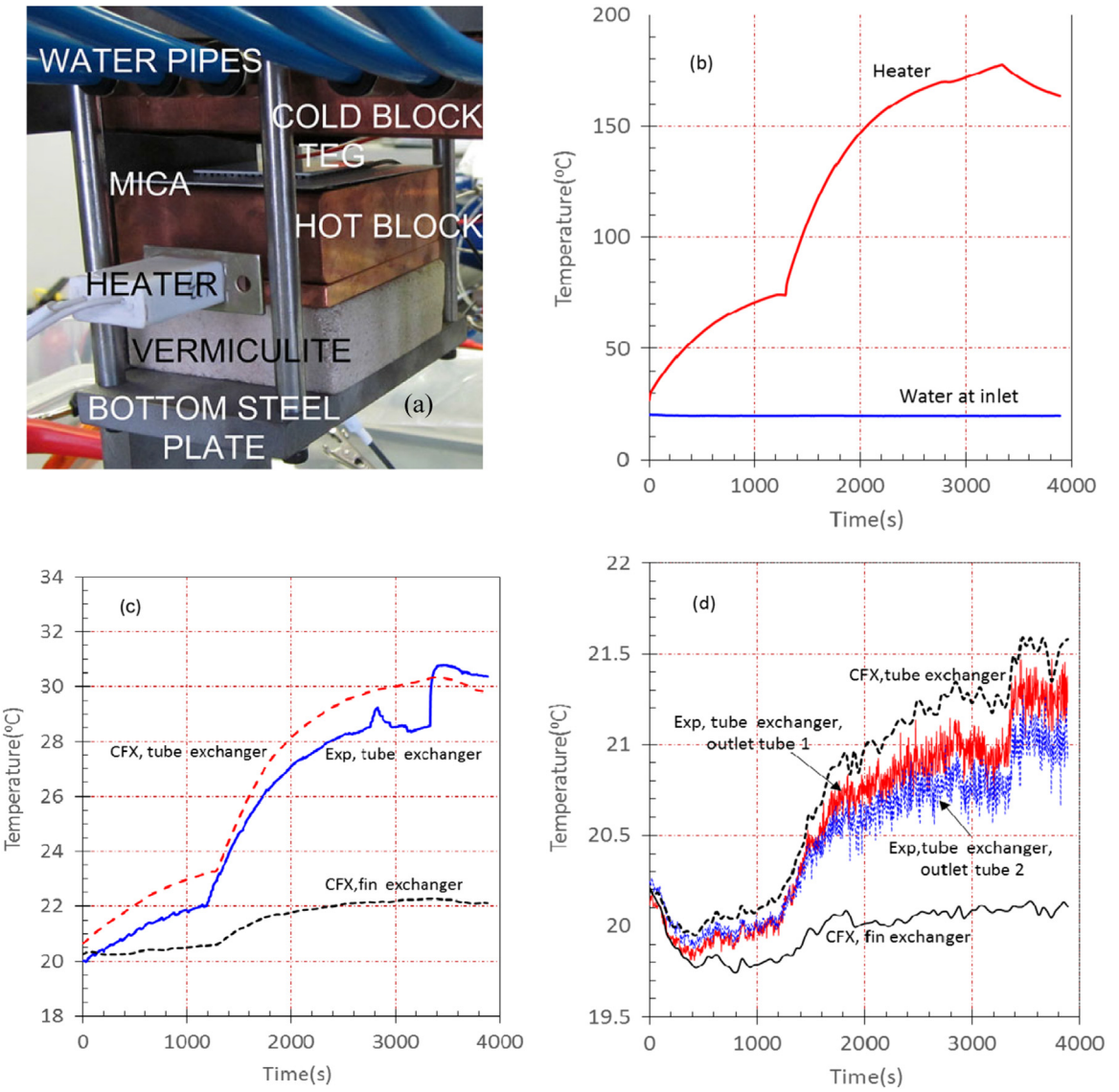

Fig. 4. Experimental setup, given temperature profiles and predicted temperature curves, (a) photo of setup, (b) input temperature, (c) predicted temperature on the cold side of TEG, (d) predicted temperature of water at the outlet of heat exchanger.

in the fin heat exchanger, thus indicating that this heat exchanger is effective in maintaining the TEG cold side in a lower temperature compared with the tube exchanger.

In the next sections, we will focus on the steady thermal fluid dynamics and performance of the two heat exchangers under a variable cooling water flow rate while keeping the heater at a constant temperature.

3.2. Thermal and hydraulic performance

The change in temperature difference between the water at the inlet of the exchanger and the TEG cold side surface, and the pressure drop across the two heat exchangers are illustrated in Fig. 6. The heater is subject to 175 °C temperature. The two exchangers share nearly the same pressure drop. However, the temperature rise in the fin exchanger is less than that in the tube exchanger, especially at a flow rate lower than 2 L/min. This is not surprising because the area of the interface between the water and solid walls for exchanging heat in the fin exchanger is 30.6 times larger than that in the tube exchanger.

The specific temperature difference/rise, i.e. the temperature rise per Watt is illustrated in Fig. 7(a), represents the thermal resistance of the heat exchanger. Thus the lower the specific temperature rise on the cold side, the better the thermal performance and the more the heat is taken away by the cooling water. Further, the specific temperature rise remains unchanged when the temperature of the heater is either 175 °C, 200 °C or 250 °C. The reason for this is that the

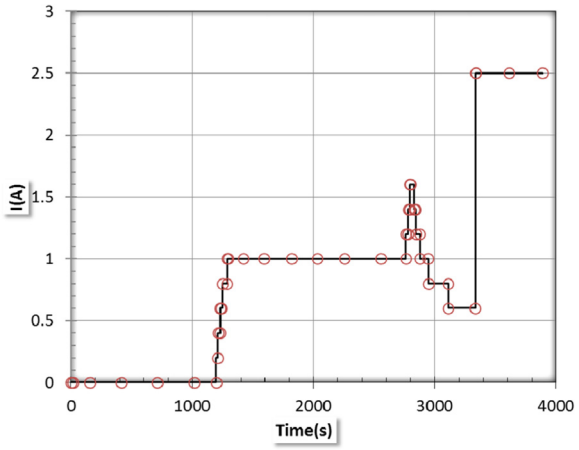

Fig. 5. Electrical current time history applied in TEG performance characterising experiments conducted by Montecucco and Knox [12].

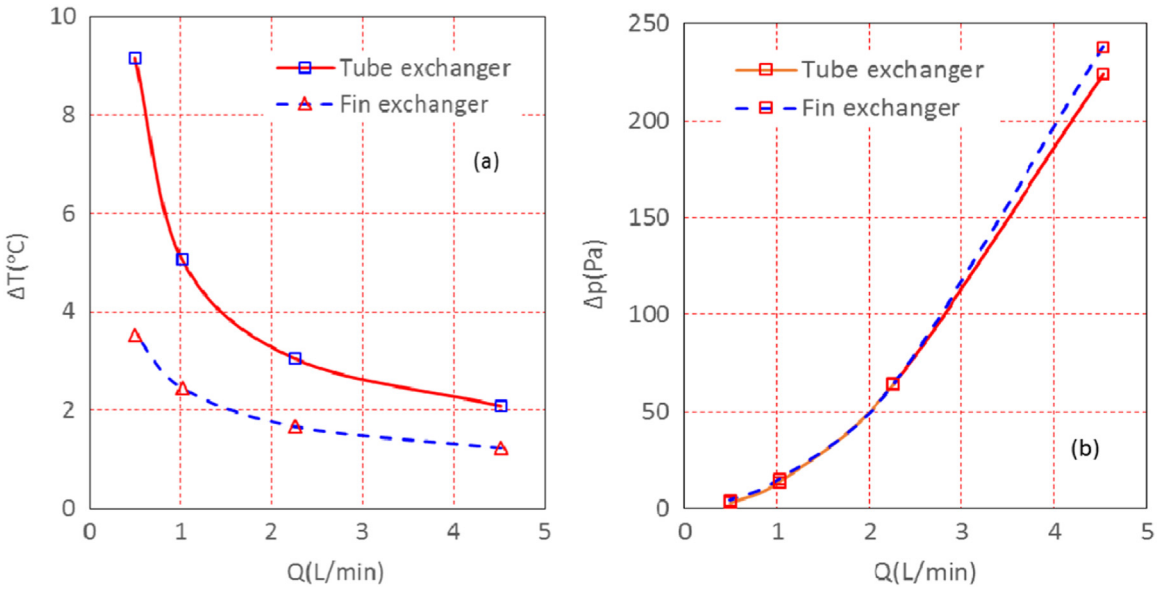

Fig. 6. Temperature rise and pressure drop across the heat exchangers, (a) temperature rise, (b) pressure drop.

thermal property of cooling water is constant thus remains independent of temperature in the simulations. In that case, the specific temperature difference/rise on the cold side is an important thermal performance variable. By using it the temperature on the cold side of a TEG can be predicted based on the electrical power generated by the TEG.

In Esarte et al. [3], the overall heat transfer coefficients of a heat exchanger-TEG system were reported as 2.07, 2.094 and 1.72 W/°C for spiral, zig-zag and straight fin heat exchangers. This suggests that the thermal resistances of these exchangers are 0.483, 0.478 and 0.581 °C/W respectively. These values are larger than the thermal resistances shown in Fig. 7. Thus the two heat exchangers designed by the authors, especially the fin exchanger, are better than these three heat exchangers in terms of the thermal performance.

According to [12], the cooling water flow rate is 1.02 L/min (17 g/s) for the tube heat exchanger. Obviously, this flow rate may be improper because it can result in a 4.5 °C temperature rise, see Fig. 6(a). Thus the results suggest that the optimal working flow rate should be 2 L/min to get a smaller temperature rise and pressure drop for the fin heat exchanger, because when the flow rate is beyond 3 L/min, the pressure drop increases rapidly.

3.3. *Temperature and flow patterns*

The temperature contours on the TEG complete system are shown in Fig. 8 for both heat exchangers when the heater is

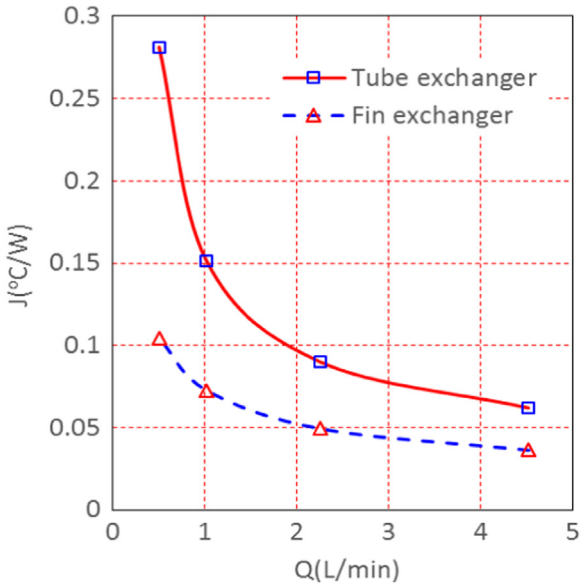

Fig. 7. Specific temperature rise across the two heat exchangers.

at 250 °C temperature and the cooling water flow is at 2.26 L/min. It is seen that the TEG system has the highest temperature heat source and the lowest temperature heat sink, with a very large temperature gradient across the TEG itself. The two heat exchangers are able to maintain a low heat sink temperature to establish a temperature difference across the TEG, generating electricity. A similar temperature contour is found with other heater temperatures and water flow rates.

The temperature contours on the cooling water surfaces and cold side of TEG are shown in Fig. 9 when the heater is at 175 °C temperature and the cooling water is running at 2.26 L/min flow rate. Clearly, the fin exchanger is subject to a lower and more uniform temperature profile compared with the tube exchanger.

For the fin heat exchanger, the temperature of cooling water at various flow rates and heater temperatures is shown in Fig. 10. The highest temperature reduction occurs with increasing flow rate and lowering heater temperature. Its position is slightly downstream and off the heat exchanger centre.

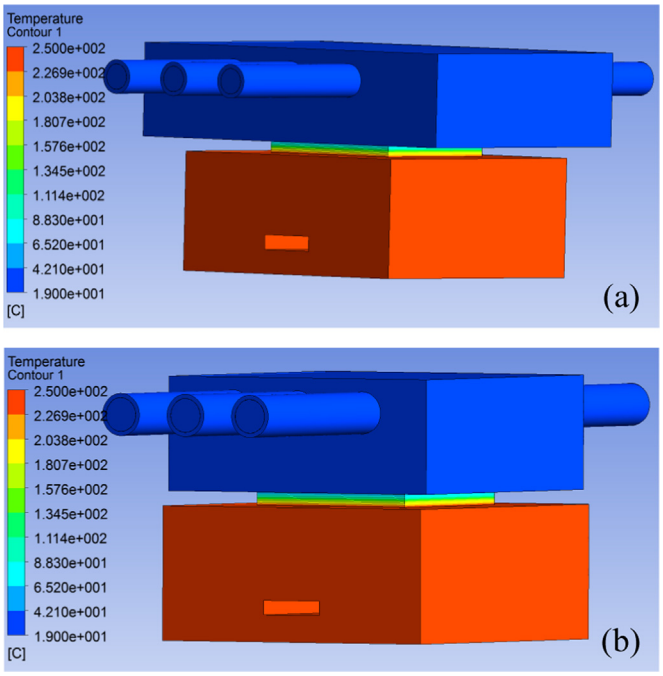

Fig. 8. Temperature contours on the whole TEG system when the heater is at 250 °C temperature and the cooling water is flowing at 2.26 L/min flow rate in two heat exchangers, (a) tube exchanger, (b) fin exchanger.

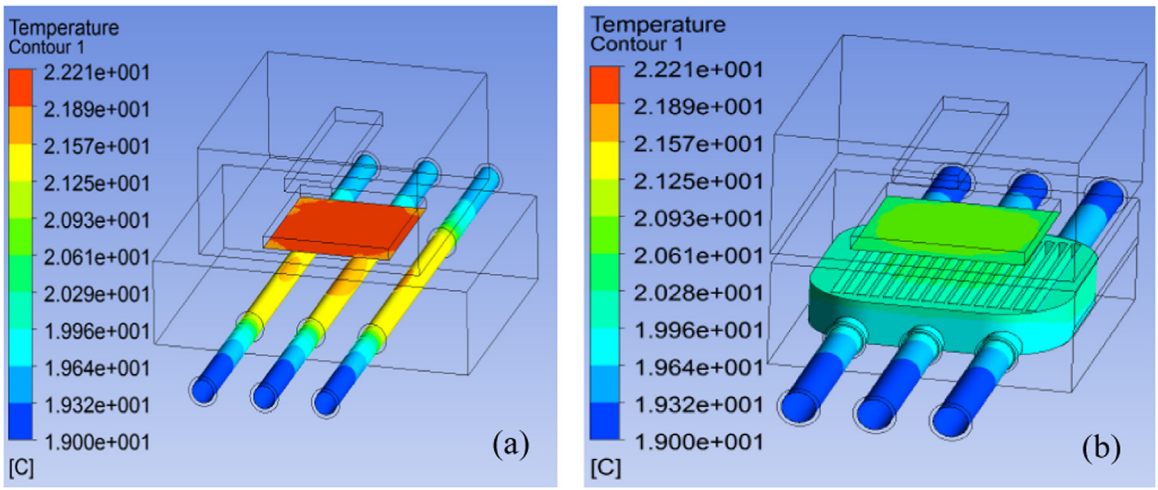

Fig. 9. Temperature contours on cooling water surfaces and TEG cold side of both heat exchangers at 175 °C temperature in the heater and 2.26 L/min cooling water flow rate, (a) tube exchanger, (b) fin exchanger.

Under 175 °C and 2.26 L/min working conditions, the cooling streamlines in the two exchangers are demonstrated in Fig. 11. The streamlines are still regular in the fin heat exchanger eventhough there are vortices in the forward-facing step at the entry of an outlet pipe. In fact, when the flow rate is as low as 1.02 L/min, the vortex pattern is established as shown in Fig. 12. To eliminate the unwanted vortex pattern, the geometrical shape of the entry to the outlet pipe of the fin heat exchanger needs to be improved.

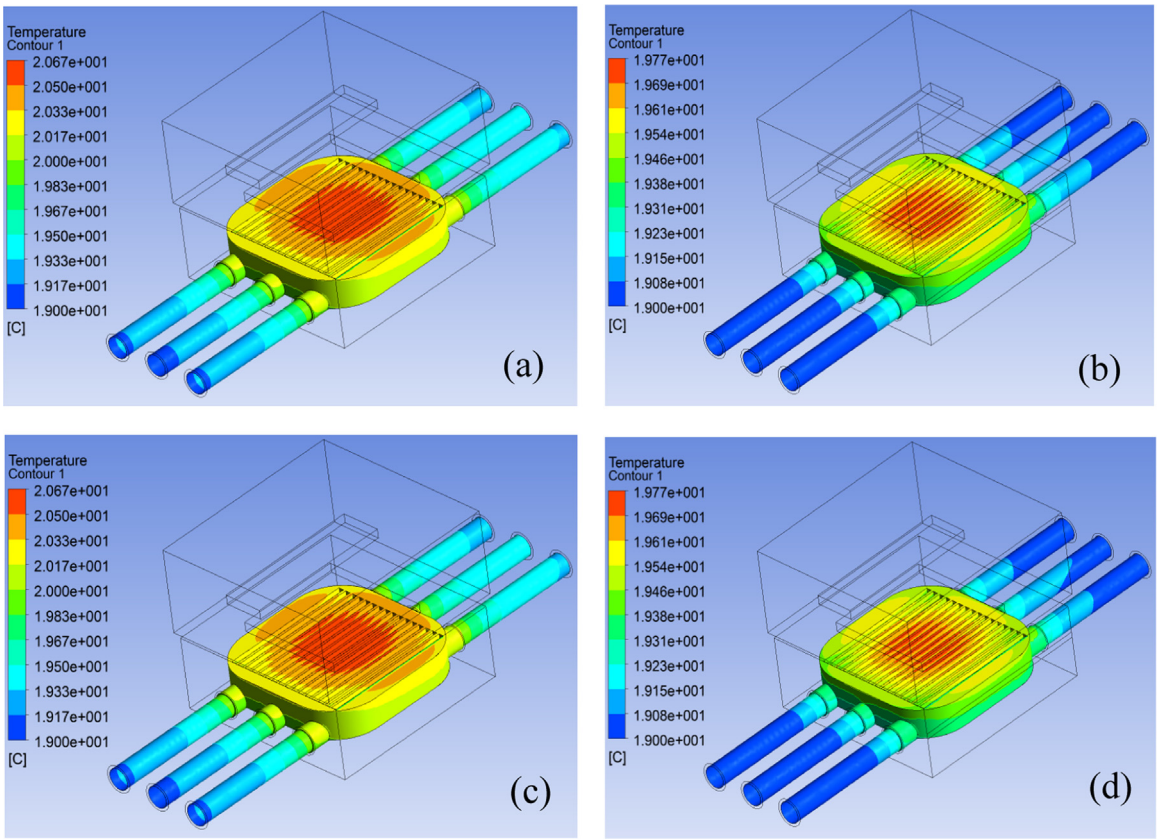

Fig. 10. Temperature of cooling water in fin heat exchanger at various flow rates and heater temperatures, (a) 200 °C and 2.26 L/min, (b) 200 °C and 9.05 L/min, (c) 250 °C and 2.26 L/min, (d) 250 °C and 9.05 L/min.

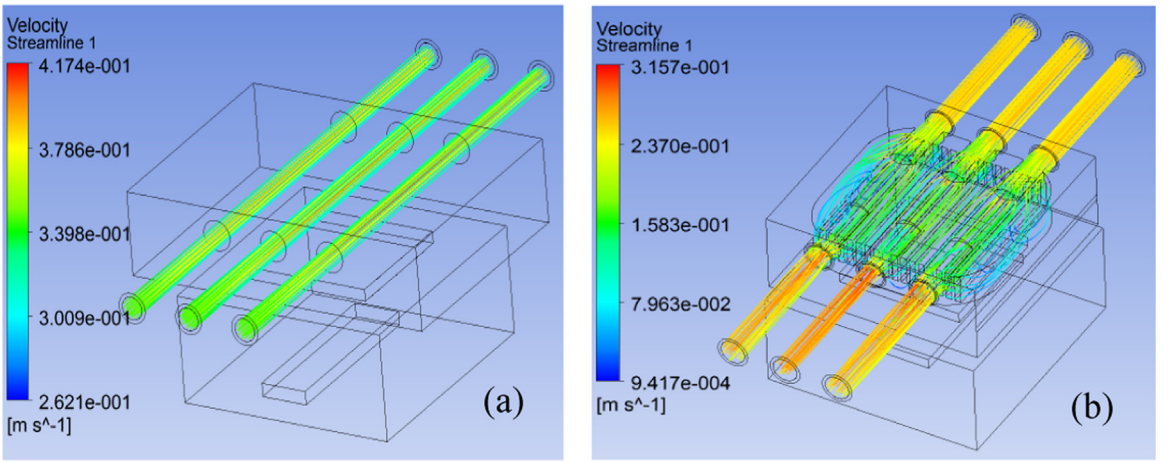

Fig. 11. Streamlines in both heat exchangers at 175 °C temperature in the heater and 2.26 L/min cooling water flow rate, (a) tube exchanger, (b) fin exchanger.

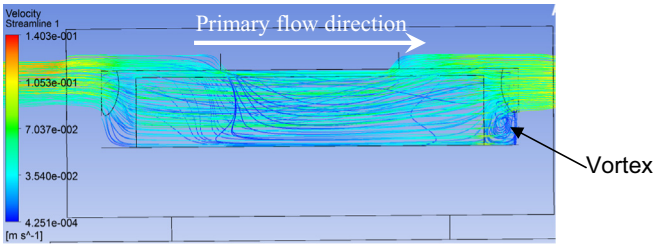

Fig. 12. Streamlines in fin heat exchange at 250 °C temperature in the heater and 1.02 L/min (Re = 767) cooling water flow rate.

3.4. Discussion

The Reynolds number of the two heat exchangers depends on the cooling water flow rate when the cooling water density and viscosity are fixed. Fig. 13 illustrates the Reynolds number of the two exchangers, which is plotted as a function of the flow rate. The Reynolds number is defined based on the water inlet velocity, tube inner diameter and water viscosity at 19 °C as,

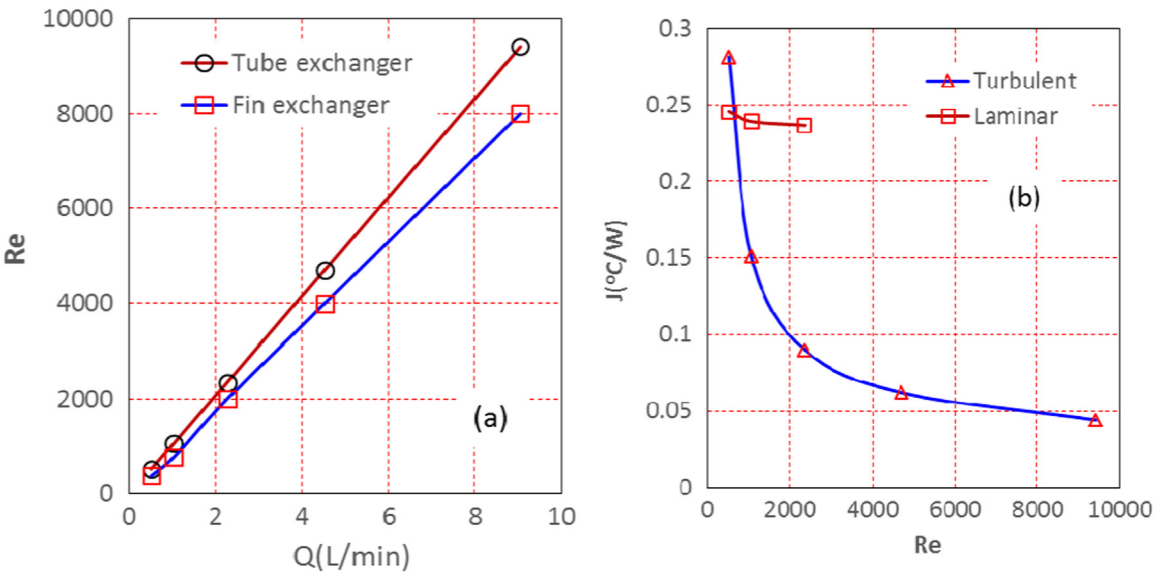

Fig. 13. Reynolds number of inlet tube of two heat exchangers is terms of flow rate (a) and the specific temperature rise is as a function of Reynolds number in tube heat exchanger based on turbulent and laminar flow models, respectively (b).

$$\mathrm{Re} = \frac{4Q}{\pi d\nu} \tag{4}$$

where d is the inner diameter of an inlet tube, 10 mm, Q and ν are the flow rate of water and its kinetic viscosity at 19 °C respectively.

For the fin heat exchanger, this number may not represent the true Reynolds number. This is due to uneven flow in the fin heat exchanger between fin channel, and it is out-with the scope of this work define such a Reynolds number inside the exchanger. However, if we assume that the flow is uniformly distributed in various fin channels, then the apparent Reynolds number can be defined and evaluated. In this context, the apparent Reynolds number of a fin heat exchange is written as

$$\mathrm{Re}_{fin} = \frac{Q}{(n+1)(h \times s)} \times \frac{4(h \times s)}{2(h+s)\nu} \tag{5}$$

where h is the height of fins, 10 mm, s is the space between two neighboring fins, 1 mm and n is the number of fins, 46. Since $h \gg s$, $h + s \approx h$, the apparent Reynolds number is approximated by the following

$$\mathrm{Re}_{fin} = \frac{2Q}{(n+1)h\nu} \tag{6}$$

The ratio of the two Reynolds numbers is expressed by the following equation

$$\frac{\mathrm{Re}}{\mathrm{Re}_{fin}} = \frac{2}{\pi}\frac{(n+1)h}{d} = 30 \tag{7}$$

This therefore implies that the tube Reynolds number is 30 times the apparent Reynolds number of the fin heat exchanger.

It is also seen that when the flow rate is less than 2.0 L/min the Reynolds number is less than 2000, indicating the flow regime in the two exchangers may be laminar. Unfortunately, if the flow model is switched to the laminar one, the specific temperature rise does not seem to be reasonable, see Fig. 13(b). Thus the turbulent flow model is applied in all the heat transfer simulations.

In the heat transfer simulations, the cooling water physical property is constant. To identify the effects of variable property on the heat transfer and pressure drop, the cooling water property constants are correlated with the water temperature and implemented accordingly in the simulations. Because the cooling water temperature rise is less than 10 °C, the effects of the property constants on pressure drop and specific temperature rise are negligible.

Even though the fin heat exchanger has exhibited much better thermal performance over the tube heat exchanger, the former is subject to an expensive manufacturing cost. It is advised that cheaper manufacturing methods for the fin heat exchanger are found.

Also noted is that the fin heat exchanger is not as rigid as the tube heat exchanger because the fin exchanger is like a hollow structure. To evaluate the deformation of the fin exchanger under a compression of a load, a finite element analysis is desirable. Otherwise, a new method to firmly attach the TEG to the heat exchanger needs to be developed.

4. Conclusion

The thermal parameters (heat transfer and fluid flow) were investigated and compared in both tube and fin heat exchangers using ANSYS CFX 15.0 under the same working conditions. Several issues such as the Reynolds number and effects of variable water property on the specific temperature rise have been discussed. The two heat exchangers exhibit a better thermal performance compared with the existing correlation of heat exchangers for TEG applications. Furthermore, the fin heat exchanger is more compact and thus has a better thermal performance than the tube heat exchanger. The fin heat exchanger exhibits vortex structure in the entrance to the outlet pipes. The laminar and turbulent models can result in different specific temperature rises at low Reynolds number. For further confirmation, deformation of the fin heat exchanger is needed to analyse under a compressive load by finite element analysis. Cheaper techniques for manufacturing fin exchangers are worth further investigation. Alternative methods for connecting TEG and the fin heat exchanger should also be considered. Further validation of heat transfer experiments on two kinds of heat exchangers are also desirable.

Acknowledgement

The work is supported by EPSRC SUPERGEN Solar Challenge with Grant: EP/K022156/1 - Scalable Solar Thermoelectrics and Photovoltaics (SUNTRAP).

References

[1] J. Henderson, Analysis of a heat exchanger-thermoelectric generator system, in: Proceedings of the 14th Intersociety Energy Conversion Engineering Conference, August 5–10, 1979, Boston, Massachusetts, USA.
[2] J. Yu, H. Zhao, A numerical model for thermoelectric generator with parallel-plate heat exchanger, J. Power Sources 172 (2007) 428–434.
[3] J. Esarte, M. Gao, D.M. Rowe, Modelling heat exchangers for thermoelectric generators, J. Power Sources 93 (2001) 72–76.
[4] M. Bhutta, N. Hayat, M. Bashir, A. Khan, K. Ahmad, S. Khan, CFD applications in various heat exchangers design: a review, Appl. Therm. Eng. 32 (2012) 1–12.
[5] A. Kanaris, A. Mouza, S. Paras, Optimal design of a plate heat exchanger with undulated surfaces, Int. J. Therm. Sci. 48 (2009) 1184–1195.
[6] D. Karmo, S. Ajib, A. Khateeb, New method for designing an effective finned heat exchanger, Appl. Therm. Eng. 51 (2013) 539–550.
[7] L. Sun, C.L. Zhang, Evaluation if elliptical finned-tube heat exchanger performance using CFD and response surface methodology, Int. J. Therm. Sci. 75 (2014) 45–53.
[8] E. Urbiola, Y. Vorobiev, Investigation of solar hybrid electric/thermal system with radiation concentrator and thermoelectric generator, Int. J. Photoenergy 2013 (2013) 7, http://dx.doi.org/10.1155/2013/704087.
[9] A. Sarhadi, R. Bjork, N. Lindeburg, P. Viereck, N. Pryds, A thermoelectric power generating heat exchanger: part II: numerical modeling and optimization, Energy Convers. Manag. 119 (2016) 481–487.
[10] F.P. Incropera, D.P. DeWitt, T.L. Bergman, A.S. Lavine, Fundamentals of Heat and Mass Transfer, 6th ed. John Wiley & Sons, New Jersey, 2007.
[11] ANSYS, ANSYS CFX-Solver Theory Guide, Release 15.0, ANSYS Inc., Canonsburg, PA, USA, 2013.
[12] A. Montecucco, A.R. Knox, Accurate simulation of thermoelectric power generating systems, Appl. Energy 118 (2014) 166–172.
[13] A. Montecucco, J. Buckle, J. Siviter, A.R. Knox, A new test rig for accurate nonparametric measurement and characterization of thermoelectric generators, J. Electron. Mater. 42 (2013) 1966–1973.